Revisiting the potential of alternating repetition time balanced steady state free precession imaging in the abdomen at 3T

Oliver J. Gurney-Champion[1,2], Remy Klaassen[3,4], Jaap Stoker[1], Arjan Bel[2], Hanneke W.M. van Laarhoven[3], Aart J. Nederveen[1], and Sonia I. Goncalves[5]

[1]Radiology, Academic Medical Center, Amsterdam, Netherlands, [2]Radiation Oncology, Academic Medical Center, Amsterdam, Netherlands, [3]Department of Medical Oncology, Academic Medical Center, Amsterdam, Netherlands, [4]Laboratory for Experimental Oncology and Radiobiology, Academic Medical Center, Amsterdam, Netherlands, [5]Institute for Biomedical Imaging and Life Sciences, University of Coimbra, Coimbra, Portugal

Targeted audience: Clinical scientists interested in 3D fat-saturation techniques, physicians interested in abdominal MRI

Purpose: Abdominal MR-imaging, for example in pancreatic cancer patients, is challenging as the pancreas is small, prone to respiratory motion and embedded in fat. Therefore, a fast and signal (contrast) to noise ratio (S(C)NR) effective sequence, preferably with fat saturation, is desired. A sequence that offers such properties is the alternating repetition time balanced steady state free precession (ATR-bSSFP). This 3D sequence can be obtained in a single breath hold at a high resolution and S(C)NR.[1] Furthermore, the alternation between different TRs (TR_1, TR_2), together with an adjusted RF phase cycling, modulates the frequency response function and creates broad stop-bands which can be used for inherent fat saturation.[2] Similar to bSSFP, image contrast depends on the ratio between tissue relaxation times, T_1/T_2. Despite the potential of ATR-bSSFP for clinical abdominal imaging, data acquisition strategies are still largely empirical and chosen heuristically. For example, the flip angle (FA) that yields the highest SNR, has been loosely determined for ATR-bSSFP only for $T_1/T_2<6$.[2] Furthermore, the FAs that yield the best fat saturation and contrast to noise ratio (CNR) are unknown. Therefore, the purpose of this research was to determine the optimal settings for $\tau=TR_1/TR_2$ and FA with respect to fat saturation effectiveness and CNR between abdominal tissues at 3T.

Methods: We ran Bloch simulations, using Spin-Bench,[3] to calculate ATR-bSSFP S(C)NR as function of FA (1–90°) and τ (1–3) for different T_1/T_2-ratios (3–50). We also calculated the S(C)NR of conventional bSSFP for comparison.[4] In addition, the CNR for T_1/T_2 from different abdominal organs (liver: T_1/T_2=23, pancreas: 17 and kidney cortex: 15) as function of FA and were calculated. We validated simulation results with phantom measurements on a 3T scanner. The phantom consisted of a rack with 14 tubes, one containing peanut oil and the remaining containing gels with different T_1/T_2 values (4–46).[5] The compromise between FA magnitude and SAR constraints limited the FAs to be ≤51° for τ=1, ≤35° for τ=2 and ≤21° for τ=3. We determined the effectiveness of fat saturation experimentally, by taking the ratio between the average signal from the tube containing peanut oil and the average signal of all other tubes, and compared to the fat saturation effectiveness of a Dixon sequence at FA=9°. Finally, in-vivo 3D ATR-bSSFP (1.7×1.7×2 mm^3 resolution, 400×350×95 mm^3 FOV, single breath hold of 19s) data was acquired in two healthy volunteers for different FA and values, and in one pancreatic cancer patient using the optimized parameters.

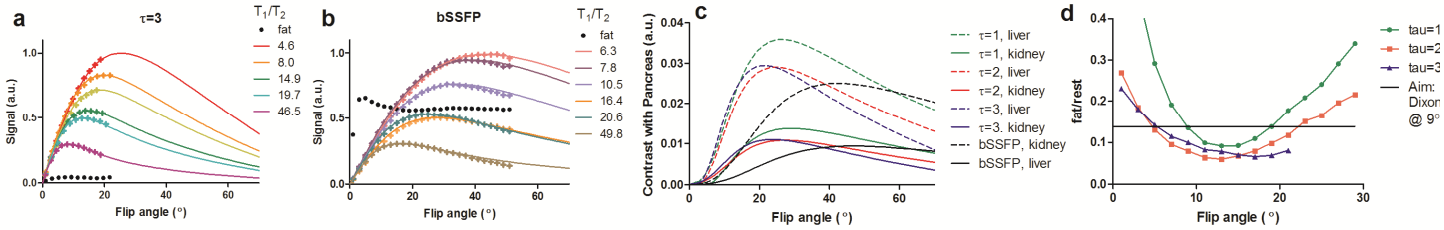

Fig 1: Measurements (crosses) and simulations (lines) of the signal as function of the FA for ATR-bSSFP τ=3 **(a)** as well as bSSFP **(b)** for different T_1/T_2. **c:** Simulated contrast between the pancreas and other organs as function of the FA for τ=1–3. **d:** Ratio of the signal from the tube containing fat, divided by the average signal from all other tubes. The black line indicates this value for Dixon with FA=9°.

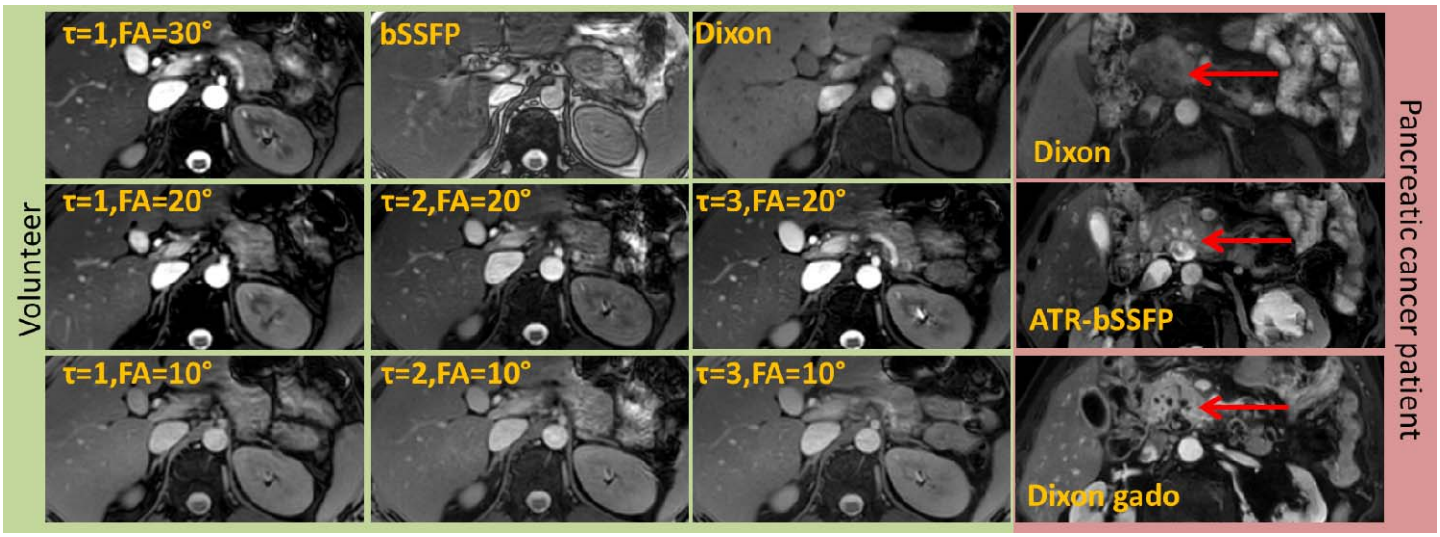

Fig 2: In-vivo ATR-bSSFP, Dixon and bSSFP images in a volunteer (green) and an ATR-bSSFP image without Gadovist compared to a Dixon image prior to and after injection of Gadovist in a pancreatic tumour patient (red). The arrow indicates the pancreas, where ATR-bSSFP had superior contrast over pre Gadovist Dixon.

Results: The simulations agreed with the measurements for all selected values of τ, FA and T_1/T_2 (Fig. 1 a, b). Simulations showed that for typical T_1/T_2 values in the abdomen, the signal as a function of FA is maximum for lower FAs for ATR-bSSFP (11.8°–18.2°) when compared to bSSFP (23.2°–29.0°). Furthermore, the FA value corresponding with maximum signal decreases with increasing τ. Simulations also showed that the FA that allows for the highest CNR varies per organ pair; for the organs investigated it was between 24–30° for τ=1, 22–28° for τ=2 and 20–24° for τ=3 for ATR bSSFP and 40–47° for bSSFP (Fig. 1c: example for pancreas). Experimentally, fat saturation effectiveness was best for τ=3 ATR-bSSFP (Fig. 1d), even outperforming fat saturation effectiveness in Dixon imaging. The in-vivo images showed the best contrast between pancreas, liver and kidneys for τ=3 and FA=20° (Fig. 2), in agreement with simulations. Due to the inherent T_2 contrast, fluid containing structures, like ductuli and cysts, were more pronounced on the ATR-bSSFP compared to the equivalent unenhanced Dixon images. In the pancreatic cancer patient, ATR-bSSFP showed structures in the pancreas as a positive contrast, which on the Dixon image only became visible as negative contrast after contrast injection (Gadovist).

Conclusion: In this study we showed that τ=3 and FA=20° yields the best compromise between contrast and f6at saturation in abdominal imaging. At these settings, the abdomen can be imaged within a breath hold at high resolution, with fat saturation and a T1/T2 contras that allows us to distinguish relevant pathological structures.

References: [1]: S.I. Gonçalves et al. Magn. Reson. Med. **67**(3), 595–600 (2012). [2]: J. Leupold et al. Magn. Reson. Med. **55**(3), 557–65 (2006). [3]: www.heartvista.com/SpinBench [4]: R.R. Ernst. Rev. Sci. Instrum. **37**(1), 93 (1966). [5]: C.M.J. de Bazelaire et al. Radiology **230**(3), 652–9 (2004).